Multiparametric Magnetic Resonance Imaging, [68]Ga Prostate-Specific Membrane Antigen Positron Emission Tomography–Computed Tomography, and Respective Quantitative Parameters in Detection and Localization of Clinically Significant Prostate Cancer in Intermediate- and High-Risk Group Patients: An Indian Demographic Study

Abstract

Objectives: The objective of this study was to evaluate the diagnostic accuracy of multiparametric magnetic resonance imaging (mpMRI) and ^{68}Ga prostate-specific membrane antigen positron emission tomography–computed tomography (PSMA PET-CT) and respective quantitative parameters (K^{trans} – influx rate contrast, K_{ep} – efflux rate constant, ADC – apparent diffusion coefficient, and SUVmax ratio – prostate SUVmax to background SUVmax ratio) in detection and localization of clinically significant prostate cancer (CSPCa) in D'Amico intermediate- and high-risk group patients (prostate-specific antigen [PSA] >10 ng/ml). **Methodology:** The study included thirty-three consecutive adult men with serum prostate specific antigen >10ng/ml, and systematic 12 core prostate biopsy proven prostate cancer. All the 33 patients, were evaluated with mpMRI, and ^{68}Ga PSMA PET-CT. The biopsy specimens and imaging were evaluated for 12 sectors per prostate by a predetermined scheme. **Results:** MpMRI Prostate Imaging Reporting and Data System version 2 (PI-RADS v2) score ≥3 showed higher sensitivity than ^{68}Ga PSMA PET-CT (96.3% vs. 82.4%), with similar specificity (54.5% vs. 54.5%) (n = 33 patients, 396 sectors). Combined use of MRI and ^{68}Ga PSMA PET-CT in parallel increased sensitivity (99.5%) and NPV (98.7%) for detection of CSPCa and combined use of MRI and ^{68}Ga PSMA PET-CT in series increased specificity (71.8%) and PPV (71.5%) (n = 33 patients, 396 sectors). ADC showed a strong negative correlation with Gleason score (r = −0.77), and the highest discriminative ability for detection and localization of CSPCa (area under curve [AUC]: 0.91), followed by K^{trans} (r = 0.74; AUC: 0.89), PI-RADS (0.73; 0.86), SUVmax ratio (0.49; 0.74), and K_{ep} (0.24; 0.66). **Conclusion:** MpMRI PI-RADS v2 score and ^{68}Ga PSMA PET-CT (individually as well as in combination) are reliable tool for detection and localization of CSPCa. Quantitative MRI and ^{68}Ga PSMA PET-CT parameters have potential to predict Gleason score and detect CSPCa.

Keywords: *[68]Ga Prostate-specific membrane antigen positron emission tomography–computed tomography, clinically significant prostate cancer, multiparametric magnetic resonance imaging, quantitative magnetic resonance imaging parameters (apparent diffusion coefficient, K^{trans}, and K_{ep}), SUVmax*

**Vijay Kubihal,
Sanjay Sharma,
Rakesh Kumar[1],
Amlesh Seth[2],
Rajeev Kumar[2],
Seema Kaushal[3],
Jayati Sarangi[3],
Ravikant Gupta[1],
Chandan Jyoti Das**

Department of Radiodiagnosis, [1]Nuclear Medicine, [2]Urology, and [3]Pathology, All India Institute of Medical Sciences, New Delhi, India

Introduction

Prostate cancer is the fourth most common cancer overall and the second most common cancer in men, with over 1.3 million new cases diagnosed world over in 2018 alone.[1] Prostate cancer incidence shows increasing trend in India.[2] The prostate cancer screening remains debatable, however, diagnosis is aided by the serum prostate-specific antigen (PSA) levels followed by the standard transrectal US-guided biopsy. The diagnostic accuracy of this method is still inefficacious and can lead to overdiagnosis and overtreatment of clinically insignificant prostate cancer.[3,4] Multiparametric magnetic resonance imaging (mpMRI) Prostate Imaging Reporting And Data System version 2 (PI-RADS v2) has good sensitivity for detection and localization of clinically significant prostate cancer (CSPCa) and can guide the patient selection for biopsy overcoming the above

How to cite this article: Kubihal V, Sharma S, Kumar R, Seth A, Kumar R, Kaushal S, *et al*. Multiparametric magnetic resonance imaging, ^{68}Ga prostate-specific membrane antigen positron emission tomography–computed tomography, and respective quantitative parameters in detection and localization of clinically significant prostate cancer in intermediate- and high-risk group patients: An Indian demographic study. Indian J Nucl Med 2021;36:362-70.

Access this article online

Website: www.ijnm.in

DOI: 10.4103/ijnm.ijnm_80_21

Quick Response Code:

limitation.[5] In addition, molecular imaging of prostate cancer also has shown good results and allows whole-body evaluation of tumor biology. Prostate-specific membrane antigen (PSMA) is a transmembrane glycoprotein expressed in all forms of prostate tissue, including prostate cancer and its over expression is associated with cancer progression and disease recurrence.[6,7] There are innumerable studies that evaluated the role of PSMA positron emission tomography (PET)/computed tomography (CT) in prostate cancer; majority of them studied its role in detection of metastases or biochemical recurrences.[8-16] Of the few studies that evaluated PSMA PET-CT in intraprostatic cancer, only a countable few evaluated its role in localization at sector level and in combination with mpMRI.[17-20]

The objectives of our study are (1) to evaluate the individual as well as combined sensitivity and specificity of mpMRI and ^{68}gallium (^{68}Ga) PSMA PET-CT in detection and localization of CSPCa in patients with intermediate and high risks for prostate cancer and (2) to evaluate the ability of quantitative MRI parameters (K^{trans} – influx rate contrast, K_{ep} – efflux rate constant, and ADC – apparent diffusion coefficient) and PSMA PET SUVmax to background ratio (SUVmax ratio) to detect and localize CSPCa and predict tumor aggressiveness.

The accurate detection and localization of prostate cancer can help in planning biopsy, reducing the false-negative results and planning minimally invasive focal therapies.

Methodology

Study design

The study was conducted at All India Institute of Medical Sciences, New Delhi, during the period between December 2016 and November 2018, with approval from the Institute Ethical Committee.

Inclusion criteria

Adult patients (above 18 years of age) with serum PSA >10 ng/ml (D'Amico intermediate and high risks for prostate cancer).[21]

Exclusion criteria

- Patients with biopsy negative for prostate cancer
- Nonconsenting patients
- Contraindications to MRI like cardiac pacemakers
- Contraindications to gadolinium administration
- Poor performance status of the patient (e.g. acute heart failure)
- History of previous treatment for diseases related to prostate.

Sample size

The sample size was 33 patients, 396 sectors.

Sixty-eight consecutive men, with serum PSA >10 ng/ml, and no contraindications to MRI, and no previous treatment for prostate cancer, were initially recruited in our study. A written informed consent, relevant clinical history was obtained from all the patients. All the patients underwent mpMRI, and ttransrectal ultrasound (TRUS) guided systematic 12-core biopsy. In 12 patients, additional sample taken by MRI ultrasound fusion biopsy were accounted for the respective sector, from which it was taken, as shown in Figure 1. Sectoral map [Figure 1] adapted in our study is to correlate imaging findings with 12 core systematic biopsy, and is different from sectoral map recommended in PI-RADS v2. In 11 patients, who had biopsy before MRI, MRI was done, 4 weeks after the biopsy. Twenty seven patients with biopsy negative for prostate cancer, and eight patients, who didn't follow up on the date of scheduled ^{68}Ga PSMA PET CT were excluded from the study. In 33 patients with biopsy positive for prostate cancer, ^{68}Ga PSMA PET-CT was done, 4 weeks after biopsy. All the 12 patients, in whom, MRI ultrasound fusion biopsy was taken, were positive for clinically significant prostate cancer, and were included in the thirty three patients who underwent PET CT. Both imaging and biopsy were done with in period of 6 weeks.

Multiparametric magnetic resonance imaging acquisition

Prostate MRI was performed in a 3 T MRI system (3T Ingenia, Philips, The Netherlands). MRI protocol included anatomical imaging (T1- and T2-weighted nonfat-saturated images) and also functional imaging (diffusion-weighted images and dynamic contrast enhancement images). For diffusion-weighted imaging, we used b values of 0 s/mm^2, 500 s/mm^2, 1000 s/mm^2, and 1500 s/mm^2. For dynamic contrast-enhanced MR imaging, T1 maps at flip angles 5º and 15º were acquired. 0.1 mmol/kg gadodiamide contrast was then administered into the antecubital vein, at the rate of 3 ml/sec using a power injector, followed by saline
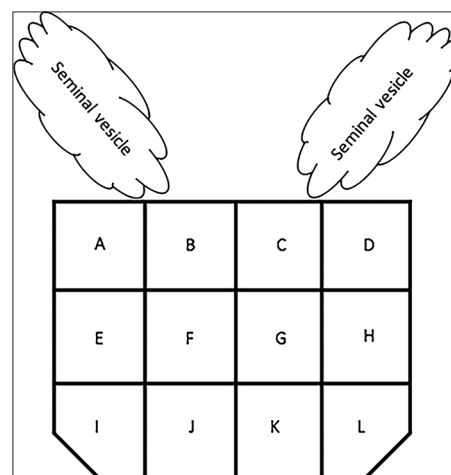

Figure 1: Schematic representation of 12 prostate sectors. (A - right lateral base, B - right medial base, C - left medial base, D - left lateral base, E - right lateral mid gland, F - right medial mid gland, G - left medial mid gland, H - left lateral mid gland, I - right lateral apex, J - right medial apex, K - left medial apex, and L - left lateral apex)

flush (20 ml). Eighty acquisitions were acquired with temporal resolution of 4.7 s. The first five images acquired before contrast injection used as a reliable baseline for analysis.

^{68}Ga-prostate-specific membrane antigen positron emission tomography–computed tomography acquisition

The patient was advised on adequate hydration on the day of the study. Each patient was administered with 74–185 MBq (2–5 mCi) ^{68}Ga-PSMA intravenously and rested for 60 min. The patient was then made to lie supine on the PET/CT scanner. An initial scout was followed by the noncontrast CT (150 mA, 120 kVp) from the vertex to the toe, and then followed by the three-dimensional emission scan, which was acquired at 2 min per bed position for the same landmarks. Images were then reconstructed using an iterative reconstruction algorithm (2 iterations, 21 subsets). Maximum intensity projection, plain PET, plain CT, and fused PET/CT images were viewed on workstation used for interpretation.

Interpretation

For interpretation, the prostate was divided into 12 prostate sectors, as shown in Figure 1.

Multiparametric magnetic resonance imaging prostate interpretation

Two radiologists in consensus interpreted mpMRI images. Both were blinded to the sectoral biopsy report. The images were evaluated on a dedicated PACS workstation (IntelliSpace Portal version 8.0, Philips, The Netherlands). PI-RADS v2 score was assigned to each of the 12 prostate zones, as shown in Figure 1. For assessment of quantitative parameters, region of interest of more than 10 mm^2 was drawn in each of these sectors. For measurement of K^{trans}, and K_{ep}, the region of interests (ROIs) were drawn over the maximum abnormality on the color map in each of the sectors. Mean K^{trans}, and K_{ep}, and ADC were noted for each of these sectors. Extended Tofts model was used for K^{trans}, and K_{ep} calculation, in the Philips IntelliSpace workstation.

^{68}Ga prostate-specific membrane antigen positron emission tomography–computed tomography interpretation

^{68}Ga PSMA PET/CT images were interpreted by two nuclear medicine physicians in consensus for the presence or absence of focally increased uptake on ^{68}Ga PSMA PET-CT in each of the 12 sectors, as shown in Figure 1. Both were blinded to the sectoral biopsy report and mpMRI report.

For quantitative analysis of SUV, regions of interest of areas more than 10 mm^2 were drawn over the maximum abnormality on the color map in each of the sectors. Values for SUVmax for each of these sectors and background SUVmax (over the gluteal muscle) were noted. For standardization, SUVmax of each of these sectors to background SUVmax ratio (SUVmax ratio) were calculated.

Histopathological examination

Biopsy sample was interpreted by two pathologists in consensus. Both were blinded to the ^{68}Ga PSMA PET/CT and mpMRI report. Biopsy specimens from each of the 12 sectors described in Figure 1, were assessed for the presence and absence of prostate cancer. If the specimen showed the presence of prostate cancer, then the Gleason score of the same was noted. Finally, based on Gleason score, biopsy-positive prostate cancer was further classified as CSPCa if the Gleason score was equal to or more than 7.

Statistical analysis

STATA 14.1 (StataCorp. 2015. Stata Statistical Software: Release 14. College Station, TX: StataCorp LP.) software was used for statistical analysis. Qualitative variables were expressed as frequencies, and continuous quantitative variables were expressed as mean and standard deviation/95% confidence interval (CI).

Diagnostic accuracy of the PI-RADS v2 (cutoff of score $\geq$3) and also ^{68}Ga PSMA PET-CT for detection of CSPCa were assessed. Diagnostic accuracy for detection of CSPCa was also assessed for combined use of mpMRI and ^{68}Ga PSMA PET-CT, both, in parallel (where result is taken positive, if either, PI-RADS score is $\geq$3 or ^{68}Ga PSMA PET-CT shows focally increased uptake) and in series (where result is taken positive, if both, PI-RADS score is $\geq$3 and ^{68}Ga PSMA PET-CT shows focally increased uptake). Quantitative parameters (ADC, K^{trans}, K_{ep}, and SUVmax ratio) were then evaluated for their correlation with Gleason score using Spearman rank correlation coefficient and for their discriminative ability in detection of CSPCa using receiver operating characteristic (ROC) curve analysis with suggestion of optimal cutoff for each the quantitative parameters, which showed good sensitivity and specificity, without compromise in either.

Results

The age of our study population (n = 33 patients) ranged between 49 years and 77 years of age, with a mean of 67.2 years (standard deviation: 6 years). The serum PSA ranged between 10.07 ng/ml and 161.58 ng/ml, with a mean of 36.46 ng/ml (standard deviation: 32.80 ng/ml). Among 33 patients included in our study, 15 patients belonged to intermediate risk group with serum prostate specific antigen between 10.1 to 20, and 18 patients belonged to high risk group with serum prostate specific antigen >20. Of the 396 sectors analyzed, 187 sectors were positive for CSPCa.

Diagnostic accuracy of multiparametric magnetic resonance imaging and ^{68}Ga prostate-specific membrane antigen positron emission tomography–computed tomography in detection and localization of clinically significant prostate cancer

For detection CSPCa, the sensitivity of mpMRI PI-RADS v2 score ≥3 was 96.3% (180/187; 95% CI: 92.4%–98.5%), specificity 54.5% (114/209; 95% CI: 47.5%–61.4%), positive predictive value 65.5% (180/275; 95% CI: 59.5%–71.1%), and negative predictive value 94.2% (114/121; 95% CI: 88.4%–97.6%). Moreover, for detection CSPCa, the sensitivity of ^{68}Ga PSMA PET was 82.4% (154/187; 95% CI: 76.1%–87.5%), specificity 54.5% (114/209; 95% CI: 47.5%–61.4%), positive predictive value 61.8% (154/249; 95% CI: 55.5%–67.9%), and negative predictive value 77.6% (114/147; 95% CI: 69.9%–84%) (n = 33 patients, 396 sectors).

Diagnostic accuracy of combined use of multiparametric magnetic resonance imaging and ^{68}Ga prostate-specific membrane antigen positron emission tomography–computed tomography in detection and localization of clinically significant prostate cancer

We observed that combined use of mpMRI (cutoff PI-RADS score ≥3) and ^{68}Ga PSMA PET-CT in parallel (where result is taken positive, if either, PI-RADS score is ≥3 or ^{68}Ga PSMA PET-CT shows significant uptake), results in increase in sensitivity (99.5% [186/187]; 95% CI: 97.1%–100%) and negative predictive value (98.7% [78/79]; 95% CI: 93.1%–100%) with reduction in specificity (37.3% [78/209]; 95% CI: 30.7%–44.3%) and positive predictive value (58.7% [186/317]; 95% CI: 53%–64.1%) for detection CSPCa. Moreover, combined use of mpMRI (cutoff PI-RADS score ≥3) and ^{68}Ga PSMA PET-CT in series (where result is taken positive, if both, PI-RADS score is ≥3 and ^{68}Ga PSMA PET-CT shows significant uptake), results in increase in specificity (71.8% [150/209]; 95% CI: 65.1%–77.8%) and positive predictive value (71.5% [148/207]; 95% CI: 64.8%–77.5%) with reduction in sensitivity (79.1% [148/187]; 95% CI: 72.6%–84.7%) and negative predictive value (79.4% [150/189]; 95% CI: 72.9%–84.9%) for detection of CSPCa.(n = 33 patients, 396 sectors).

Evaluation of quantitative parameters

Two patients were not included in analysis of quantitative dynamic contrast-enhanced MRI parameters (K^{trans}, and K_{ep}), as the acquired data were incompatible for IntelliSpace workstation to analyze, due to patient motion during contrast study. Therefore, 31 patients were available for analysis of dynamic contrast-enhanced MRI parameters (K^{trans} and K_{ep}). Both ADC and SUVmax ratio were evaluated for all the 33 patients.

Table 1 demonstrates the mean (and 95% CI) of quantitative parameters (ADC, K^{trans}, K_{ep}, and SUVmax ratio) for the sectors with and without CSPCa.

Observed difference in quantitative parameters in sectors with and without CSPCa was statistically significant ($P < 0.001$).

Spearman correlation coefficient between quantitative parameters and Gleason score showed a strong negative correlation for ADC (−0.77), strong positive correlation for K^{trans} (0.74), and PI-RADS v2 score (0.73), moderate positive correlation for SUVmax ratio (0.49), and weak positive correlation for K_{ep} (0.24). Figure 2 shows the box plots of distribution of ADC, K^{trans}, K_{ep}, and SUVmax ratio against Gleason score.

Table 2 and Figure 3 demonstrates ROC curve analysis with area under curve (AUC), suggested optimal cutoff, and corresponding sensitivity, and specificity of the quantitative parameters for detection of CSPCa.

ADC showed maximum discriminative ability for detection of CSPCa (AUC: 0.91) with suggested optimal cutoff of 0.74×10^{-3} mm²/sec and corresponding sensitivity and specificity of 86.6% and 84.2%, followed by K^{trans} (AUC: 0.89), PI-RADS (AUC: 0.86), and SUVmax ratio (AUC: 0.74). K_{ep} showed the lowest discriminative ability (AUC: 0.66).

Figure 4 shows PI-RADS 5 lesion with corresponding increased ^{68}Ga PSMA PET uptake in a patient with biopsy-proven CSPCa, and corresponding quantitative parameters.

Discussion

Diagnostic accuracy of multiparametric magnetic resonance imaging and ^{68}Ga prostate-specific membrane antigen positron emission tomography–computed tomography for detection of clinically significant prostate cancer

In our study, we observed that both mpMRI PI-RADS v2 score ≥3 and ^{68}Ga PSMA PET-CT, are reliable tool in identification of CSPCa with mpMRI showing better sensitivity and negative predictive value than ^{68}Ga PSMA PET with similar specificity and positive predictive value.

Table 1: Mean (and standard deviation) of quantitative parameters (apparent diffusion coefficient, K^{trans}, K_{ep}, and maximum standardized uptake value ratio) for the sectors with and without clinically significant prostate cancer

Parameter	Clinically significant prostate cancer	No clinically significant prostate cancer
ADC ($\times10^{-3}$ mm²/s) (n=33 patients, 396 sectors)	0.62 (0.16)	1.00 (0.27)
K^{trans} ($\times10^{-3}$ min^{-1}) (n=31 patients, 372 sectors)	24.50 (6.25)	14.92 (6.42)
K_{ep} ($\times10^{-3}$ min^{-1}) (n=31 patients, 372 sectors)	451.37 (146.22)	362.94 (181.81)
SUVmax ratio (n=33 patients, 396 sectors)	13.84 (14.28)	5.52 (4.53)

SUVmax=Maximum standardized uptake value, ADC=Apparent diffusion coefficient
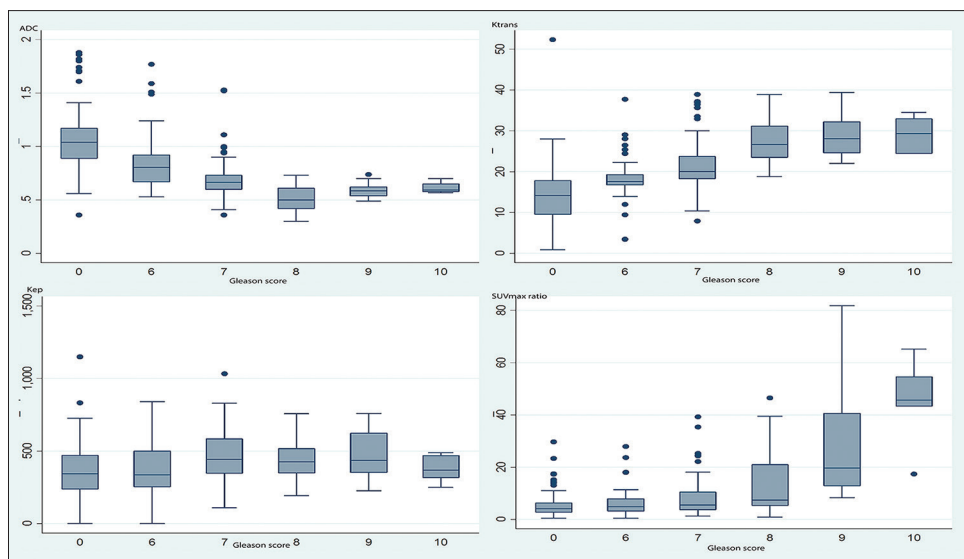
Figure 2: Box plots to show distribution of ADC, K^{trans}, K_{ep}, and SUVmax ratio against Gleason score (ADC = Apparent diffusion coefficient, K^{trans} = influx rate constant, K_{ep} = efflux rate constant, SUV = Standardized uptake value)
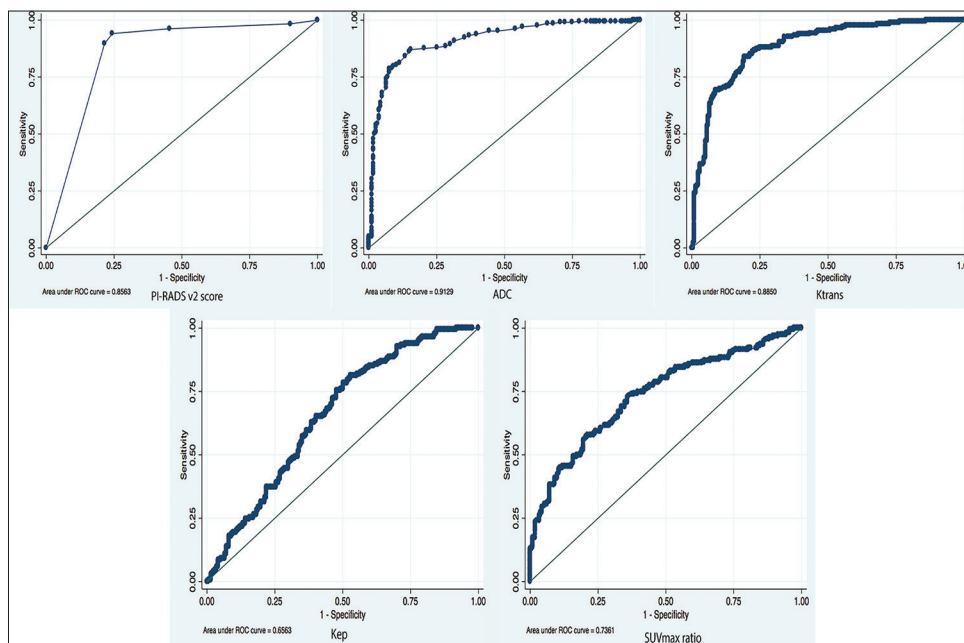

Figure 3: Receiver operating characteristic curves for PI-RADS v2 score, ADC, K^{trans}, K_{ep}, and SUVmax ratio (PI-RADS v2 = Prostate Imaging Reporting and Data System version 2, ADC = Apparent diffusion coefficient, K^{trans} = influx rate constant, K_{ep} = efflux rate constant. SUV = Standardized Uptake Value)

A variety of similar studies show wide variation in sensitivity and specificity of PI-RADS scoring system and ⁶⁸Ga PSMA PET-CT in identification of CSPCa.[17-19,22-29] In these studies, we observe that, for detection of CSPCa, PI-RADS v2 sensitivity ranged between 44% and 93% and specificity ranged between 38% and 94%, and ⁶⁸Ga PSMA PET-CT sensitivity ranged between 49% and 78.4%, and specificity ranged between 81% and 95%. Wide variation in sensitivity and specificity can be attributed to different acquisition protocols, different cutoffs used, different reference standards used, biopsy inaccuracies, and varied experience of users with PI-RADS v2.

Diagnostic accuracy of combined use of multiparametric magnetic resonance imaging and ⁶⁸Ga prostate-specific membrane antigen positron emission tomography–computed tomography for detection of clinically significant prostate cancer

Combined use of mpMRI (cutoff PI-RADS score ≥3) and ⁶⁸Ga PSMA PET-CT in parallel, results in increase in sensitivity and negative predictive value. This could be particularly helpful in selection of the patients in screening setting before biopsy, where high sensitivity is required. Combined use of mpMRI (cutoff PI-RADS score ≥3) and ⁶⁸Ga PSMA PET-CT in series, results in increase in
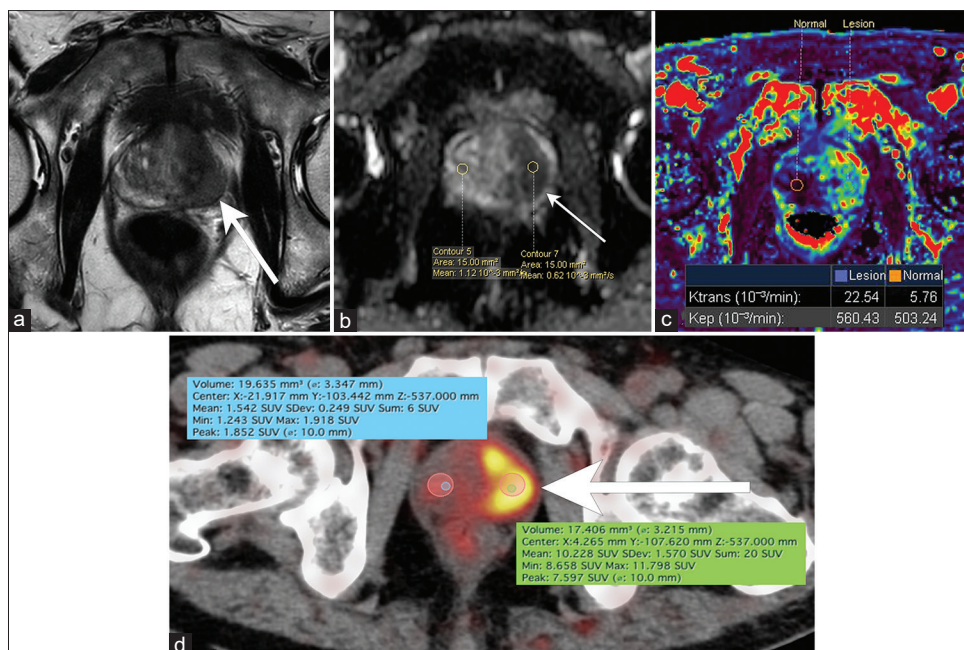
Figure 4: A 63-year-old male with obstructive lower urinary tract symptoms and increased serum prostate-specific antigen (10.06 ng/ml). Magnetic resonance imaging shows PIRADS 5 lesion in the left medial and lateral sectors of prostate base with the corresponding histopathology suggestive of prostate cancer of Gleason score 7 (4 + 3). (a) Nonfat-saturated T2-weighted axial image at prostate base shows irregular homogeneous hypointense lesion in the left medial and lateral sectors (involving both transitional zone and peripheral zone), measuring more than 1.5 cm in the longest dimension. (b) Axial apparent diffusion coefficient maps at the same level show the lesion to be focal and markedly hypointense. (c) Axial K^{trans} color map at the same level shows the lesion as focal abnormality in color map. (d) Axial ^{68}Ga positron emission tomography–computed tomography at the same level shows focal increased uptake. (b-d) ROI drawn over the above lesion on the left side (showing clinically significant prostate cancer on histopathology) shows apparent diffusion coefficient, K^{trans}, K_{ep}, and SUVmax of 0.62×10^{-3} mm²/sec, 22.54×10^{-3}/min, 560.43×10^{-3}/min, and 7.59, respectively; and ROI drawn on the right side with normal MR imaging (and no clinically significant prostate cancer on corresponding histopathology) shows apparent diffusion coefficient, K^{trans}, K_{ep}, and SUVmax of 1.12×10^{-3} mm²/sec, 5.76×10^{-3}/min, 503.24×10^{-3}/min, and 1.85, respectively. Here, we notice that apparent diffusion coefficient value is lower, and K^{trans}, and SUVmax are higher, in the sector with clinically significant prostate cancer compared to that in the sector with no clinically significant prostate cancer

Table 2: Receiver operating characteristic curve analysis with area under curve, optimal cutoff, and corresponding sensitivity, and specificity of the quantitative parameters for detection of clinically significant prostate cancer

Parameter	AUC	Optimal cutoff	Sensitivity (%)	Specificity (%)
ADC (*n*=33 patients, 396 sectors)	0.91	0.74 (×10⁻³ mm²/sec)	86.6 (162/187; 95% CI: 80.9-91.2)	84.2 (176/209; 95% CI: 78.5-88.9)
Ktrans (*n*=31 patients, 372 sectors)	0.89	18.76 (×10⁻³ min⁻¹)	84 (147/175; 95% CI: 77.7-89.1)	80.7 (159/197; 95% CI: 74.5-86)
Kep (*n*=31 patients, 372 sectors)	0.67	395 (×10⁻³ min⁻¹)	62.9 (110/175; 95% CI: 55.2-70)	60.9 (120/197; 95% CI: 53.7-67.8)
SUVmax ratio (*n*=33 patients, 396 sectors)	0.74	5.4	69 (129/187; 95% CI: 61.8-75.5)	66 (138/209; 95% CI: 59.2-72.4)

SUVmax=Maximum standardized uptake value, ADC=Apparent diffusion coefficient, AUC=Area under curve, CI=Confidence interval

specificity and positive predictive value. This is particularly useful in precise sectoral localization for biopsy target. Although, prostate cancer is often multifocal disease, a single index lesion, which is largest and most aggressive clinically significant focus of prostate cancer, drives the disease progression in most cases.[30,31] The higher positive predictive value of combined use of mpMRI and ^{68}Ga PSMA PET CT in series, along with higher spatial resolution of MRI, may be useful in selecting index lesion for the focal therapies. However, the cost and availability of PET CT may limit its wider usage.

To the best of our knowledge, there are limited studies that evaluated combined use of MRI and ^{68}Ga GSMA PET-CT for intraprostatic localization of prostate cancer. Similar study

conducted by Rhee *et al.*,[19] observed sensitivity of 38% (our study: 85.4%) and positive predictive value of 95% (our study: 82.6%) for combined use of mpMRI and PET/CT in series.

Evaluation of quantitative parameters

In our study, we observed that ADC had best correlation with tumor grade (Gleason score) and best discriminative ability for detection of CSPCa followed by K^{trans}, PI-RADS v2 score, and SUVmax ratio. K_{ep} had a weak correlation with Gleason score and poor discriminative ability for detection of CSPCa.

Table 3 demonstrates studies which evaluated the various quantitative parameters and their respective correlation coefficients with Gleason score.

Table 3: Studies which evaluated the various quantitative parameters and their respective correlation coefficients

Studies	Reference standard	ADC	K^{trans}	K_{ep}	SUVmax ratio
Ma *et al.*[32]		−0.714	−0.249	−0.126	
Wei *et al.*[33]	Radical prostatectomy + biopsy	-	0.623	-	-
Berger *et al.*[34]	Radical prostatectomy	-	-	-	0.51
Uribe *et al.*[35]	Radical prostatectomy	−0.77	-	-	-
Li *et al.*[36]	Prostate biopsy	−0.54	-	-	-
Peng *et al.*[37]	Radical prostatectomy	−0.30	0.38	-	-
Oto *et al.*[38]	Radical prostatectomy	−0.38	-	-	-
Present study	Prostate biopsy	−0.77	0.74	0.24	0.49

SUVmax=Maximum standardized uptake value, ADC=Apparent diffusion coefficient

Table 4: Studies which evaluated the various quantitative parameters and their respective discriminative abilities to differentiate sectors with and without clinically significant prostate cancer

Study	Reference standard	ADC	K^{trans}	K_{ep}	SUVmax ratio
Ma *et al.*[32]	Prostate biopsy	0.914	0.819	0.831	
Chatterjee *et al.*[39]	Radical prostatectomy	0.80 (PZ)	0.74 (PZ)	0.67 (PZ)	-
		0.45 (TZ)	0.82 (TZ)	0.79 (TZ)	
Wei *et al.*[33]	Radical prostatectomy + biopsy	-	0.764	0.778	-
Donato *et al.*[17]	Radical prostatectomy	-	-	-	0.817
Hötker *et al.* (2016)[40]	Radical prostatectomy	0.69	0.71	-	-
Vos *et al.*[41]	Radical prostatectomy	0.82 (PZ)	0.77 (PZ)	0.81 (PZ)	-
		0.65 (TZ)	0.63 (TZ)	0.80 (TZ)	
Peng *et al.*[37]	Radical prostatectomy	0.89	0.69	-	-
Kobus *et al.*[42]	Radical prostatectomy	0.81 (PZ)	-	-	-
		0.80 (TZ)			
Langer *et al.*[43]	Radical prostatectomy	0.689	0.592	-	-
Present study	Prostate biopsy	0.91	0.89	0.67	0.74

SUVmax=Maximum standardized uptake value, ADC=Apparent diffusion coefficient, PZ=Peripheral zone, TZ=Transitional zone

Table 4 demonstrates studies which evaluated the various quantitative parameters and their respective discriminative abilities for detection of CSPCa.

Wide heterogeneity observed can be attributed to differences in study design, acquisition parameters, differences in b values used, differences in the pharmacokinetic modeling used in K^{trans}, and K_{ep} maps, differences in reference standards, and expected biopsy inaccuracies.

Limitations of our study

Sample size was small (*n* = 33 patients), and thus, results may or may not represent true population statistics, requiring further validation studies with larger sample size. We used biopsy as the reference standard which is subjected to risk of inadequate and inaccurate sampling, compared to whole mount prostatectomy specimen. Also, biopsy results lack correlation with zonal anatomy of the prostate. Our histopathology results were dichotomous for the presence or absence of prostate cancer. It did not include possible causes of false-positive results in imaging for analysis (for example: prostatitis, benign prostatic hyperplasia, and atrophic changes). Hence, we had no pathological correlation of false-positive findings seen on imaging. Due to longer acquisition time, avoidance of motion artifact

was a problem. MRI data of two of our 33 patients were not suitable for quantitative analysis due to patient motion. We used PI-RADS v2 scoring system over more recent PI-RADS v2.1 during the study, however, PI-RADS v2.1 has predominant changes seen in transitional zone scoring, and lower PI-RADS score (score 1 and 2). As PI-RADS v2/v2.1 is the newly published system with limited familiarity among the radiologists, interobserver variability in various studies is probably part of a learning curve and is expected to improve as more studies get published. Higher cost for MRI and ^{68}Ga PSMA PET-CT, may limit its wider public use.

Conclusion

mpMRI PI-RADS v2 and ^{68}Ga PSMA PET-CT are both reliable tools in detection of CSPCa, with MRI having better sensitivity for detection CSPCa. Combined use of mpMRI and ^{68}Ga PSMA PET-CT in parallel will increase the sensitivity for detection of CSPCa, which could help in screening high-risk patients, where high sensitivity is required. Combined use of mpMRI and ^{68}Ga PSMA PET-CT in series will increase the specificity, and positive predictive value for detection of CSPCa, which would help in precise sectoral localization for biopsy target, and focal

therapies. Quantitative parameters, particularly ADC, and K^{trans}, provide objective and reliable method of detection of CSPCa. However, further validation studies are suggested before any clinical application of the same.

Financial support and sponsorship

Nil.

Conflicts of interest

There are no conflicts of interest.

References

1. Prostate Cancer Statistics | World Cancer Research Fund. Available from: https://www.wcrf.org/dietandcancer/cancer-trends/prostate-cancer-statistics. [Last accessed on 2020 Oct 17].
2. Hariharan K, Padmanabha V. Demography and disease characteristics of prostate cancer in India. Indian J Urol 2016;32:103-8.
3. Welch HG, Black WC. Overdiagnosis in cancer. J Natl Cancer Inst 2010;102:605-13.
4. Zlotta AR, Egawa S, Pushkar D, Govorov A, Kimura T, Kido M, *et al.* Prevalence of prostate cancer on autopsy: Cross-sectional study on unscreened Caucasian and Asian men. J Natl Cancer Inst 2013;105:1050-8.
5. Druskin SC, Macura KJ. MR imaging for prostate cancer screening and active surveillance. Radiol Clin North Am 2018;56:251-61.
6. Israeli RS, Powell CT, Corr JG, Fair WR, Heston WD. Expression of the prostate-specific membrane antigen. Cancer Res 1994;54:1807-11.
7. Ross JS, Sheehan CE, Fisher HA, Kaufman RP Jr., Kaur P, Gray K, *et al.* Correlation of primary tumor prostate-specific membrane antigen expression with disease recurrence in prostate cancer. Clin Cancer Res 2003;9:6357-62.
8. Afshar-Oromieh A, Haberkorn U, Schlemmer HP, Fenchel M, Eder M, Eisenhut M, *et al.* Comparison of PET/CT and PET/MRI hybrid systems using a 68Ga-labelled PSMA ligand for the diagnosis of recurrent prostate cancer: Initial experience. Eur J Nucl Med Mol Imaging 2014;41:887-97.
9. Eder M, Neels O, Müller M, Bauder-Wüst U, Remde Y, Schäfer M, *et al.* Novel preclinical and radiopharmaceutical aspects of [68Ga] Ga-PSMA-HBED-CC: A new PET tracer for imaging of prostate cancer. Pharmaceuticals (Basel) 2014;7:779-96.
10. Szabo Z, Mena E, Rowe SP, Plyku D, Nidal R, Eisenberger MA, *et al.* Initial evaluation of [(18) F] DCFPyL for prostate-specific membrane antigen (PSMA)-targeted PET imaging of prostate cancer. Mol Imaging Biol 2015;17:565-74.
11. Freitag MT, Radtke JP, Hadaschik BA, Kopp-Schneider A, Eder M, Kopka K, *et al.* Comparison of hybrid (68) Ga-PSMA PET/MRI and (68) Ga-PSMA PET/CT in the evaluation of lymph node and bone metastases of prostate cancer. Eur J Nucl Med Mol Imaging 2016;43:70-83.
12. Pyka T, Okamoto S, Dahlbender M, Tauber R, Retz M, Heck M, *et al.* Comparison of bone scintigraphy and 68Ga-PSMA PET for skeletal staging in prostate cancer. Eur J Nucl Med Mol Imaging 2016;43:2114-21.
13. Rowe SP, Macura KJ, Mena E, Blackford AL, Nadal R, Antonarakis ES, *et al.* PSMA-based [(18)F]DCFPyL PET/CT is superior to conventional imaging for lesion detection in patients with metastatic prostate cancer. Mol Imaging Biol 2016;18:411-9.
14. Perera M, Papa N, Christidis D, Wetherell D, Hofman MS, Murphy DG, *et al.* Sensitivity, specificity, and predictors of positive 68Ga-prostate-specific membrane antigen positron emission tomography in advanced prostate cancer: A systematic review and meta-analysis. Eur Urol 2016;70:926-37.
15. Einspieler I, Rauscher I, Düwel C, Krönke M, Rischpler C, Habl G, *et al.* Detection efficacy of Hybrid 68Ga-PSMA Ligand PET/CT in prostate cancer patients with biochemical recurrence after primary radiation therapy defined by phoenix criteria. J Nucl Med 2017;58:1081-7.
16. Bräuer A, Rahbar K, Konnert J, Bögemann M, Stegger L. Diagnostic value of additional 68Ga-PSMA-PET before 223Ra-dichloride therapy in patients with metastatic prostate carcinoma. Nuklearmedizin 2017;56:14-22.
17. Donato P, Roberts MJ, Morton A, Kyle S, Coughlin G, Esler R, *et al.* Improved specificity with 68Ga PSMA PET/CT to detect clinically significant lesions "invisible" on multiparametric MRI of the prostate: A single institution comparative analysis with radical prostatectomy histology. Eur J Nucl Med Mol Imaging 2019;46:20-30.
18. Kesch C, Vinsensia M, Radtke JP, Schlemmer HP, Heller M, Ellert E, *et al.* Intraindividual comparison of 18F-PSMA-1007 PET/CT, multiparametric MRI, and radical prostatectomy specimens in patients with primary prostate cancer: A retrospective, proof-of-concept study. J Nucl Med 2017;58:1805-10.
19. Rhee H, Thomas P, Shepherd B, Gustafson S, Vela I, Russell PJ, *et al.* Prostate specific membrane antigen positron emission tomography may improve the diagnostic accuracy of multiparametric magnetic resonance imaging in localized prostate cancer. J Urol 2016;196:1261-7.
20. Eiber M, Weirich G, Holzapfel K, Souvatzoglou M, Haller B, Rauscher I, *et al.* Simultaneous 68Ga-PSMA HBED-CC PET/MRI improves the localization of primary prostate cancer. Eur Urol 2016;70:829-36.
21. D'Amico AV, Whittington R, Malkowicz SB, Schultz D, Blank K, Broderick GA, *et al.* Biochemical outcome after radical prostatectomy, external beam radiation therapy, or interstitial radiation therapy for clinically localized prostate cancer. JAMA 1998;280:969-74.
22. Brown LC, Ahmed HU, Faria R, El-Shater Bosaily A, Gabe R, Kaplan RS, *et al.* Multiparametric MRI to improve detection of prostate cancer compared with transrectal ultrasound-guided prostate biopsy alone: The PROMIS study. Health Technol Assess 2018;22:1-176.
23. Patel NU, Lind KE, Garg K, Crawford D, Werahera PN, Pokharel SS. Assessment of PI-RADS v2 categories ≥3 for diagnosis of clinically significant prostate cancer. Abdom Radiol (NY) 2019;44:705-12.
24. Bonekamp D, Schelb P, Wiesenfarth M, Kuder TA, Deister F, Stenzinger A, *et al.* Histopathological to multiparametric MRI spatial mapping of extended systematic sextant and MR/TRUS-fusion-targeted biopsy of the prostate. Eur Radiol 2019;29:1820-30.
25. Baldisserotto M, Neto EJ, Carvalhal G, de Toledo AF, de Almeida CM, Cairoli CE, *et al.* Validation of PI-RADS v. 2 for prostate cancer diagnosis with MRI at 3T using an external phased-array coil. J Magn Reson Imaging 2016;44:1354-9.
26. Zhao C, Gao G, Fang D, Li F, Yang X, Wang H, *et al.* The efficiency of multiparametric magnetic resonance imaging (mpMRI) using PI-RADS Version 2 in the diagnosis of clinically significant prostate cancer. Clin Imaging 2016;40:885-8.
27. Lin WC, Muglia VF, Silva GE, Chodraui Filho S, Reis RB,

Westphalen AC. Multiparametric MRI of the prostate: Diagnostic performance and interreader agreement of two scoring systems. Br J Radiol 2016;89:20151056.

28. Muller BG, Shih JH, Sankineni S, Marko J, Rais-Bahrami S, George AK, *et al.* Prostate cancer: Interobserver agreement and accuracy with the revised prostate imaging reporting and data system at multiparametric MR imaging. Radiology 2015;277:741-50.

29. Abrams-Pompe RS, Fanti S, Schoots IG, Moore CM, Turkbey B, Vickers AJ, *et al.* The role of magnetic resonance imaging and positron emission tomography/computed tomography in the primary staging of newly diagnosed prostate cancer: A systematic review of the literature. Eur Urol Oncol 2021;4:370-95.

30. Hayes M, Lin-Brande M, Isharwal S. Primary focal therapy for localized prostate cancer: A review of the literature. Oncology (Williston Park) 2021;35:261-8.

31. Stabile A, Moschini M, Montorsi F, Cathelineau X, Sanchez-Salas R. Focal therapy for prostate cancer -index lesion treatment vs. hemiablation. A matter of definition. Int Braz J Urol 2019;45:873-6.

32. Ma XZ, Lv K, Sheng JL, Yu YX, Pang PP, Xu MS, *et al.* Application evaluation of DCE-MRI combined with quantitative analysis of DWI for the diagnosis of prostate cancer. Oncol Lett 2019;17:3077-84.

33. Wei C, Jin B, Szewczyk-Bieda M, Gandy S, Lang S, Zhang Y, *et al.* Quantitative parameters in dynamic contrast-enhanced magnetic resonance imaging for the detection and characterization of prostate cancer. Oncotarget 2018;9:15997-6007.

34. Berger I, Annabattula C, Lewis J, Shetty DV, Kam J, Maclean F, *et al.* ^{68}Ga-PSMA PET/CT vs. mpMRI for locoregional prostate cancer staging: Correlation with final histopathology. Prostate Cancer Prostatic Dis 2018;21:204-11.

35. Uribe CF, Jones EC, Chang SD, Goldenberg SL, Reinsberg SA, Kozlowski P. *In vivo* 3T and *ex vivo* 7T diffusion tensor imaging of prostate cancer: Correlation with histology. Magn Reson Imaging 2015;33:577-83.

36. Li L, Margolis DJ, Deng M, Cai J, Yuan L, Feng Z, *et al.* Correlation of gleason scores with magnetic resonance diffusion tensor imaging in peripheral zone prostate cancer. J Magn Reson Imaging 2015;42:460-7.

37. Peng Y, Jiang Y, Yang C, Brown JB, Antic T, Sethi I, *et al.* Quantitative analysis of multiparametric prostate MR images: Differentiation between prostate cancer and normal tissue and correlation with Gleason score – A computer-aided diagnosis development study. Radiology 2013;267:787-96.

38. Oto A, Yang C, Kayhan A, Tretiakova M, Antic T, Schmid-Tannwald C, *et al.* Diffusion-weighted and dynamic contrast-enhanced MRI of prostate cancer: Correlation of quantitative MR parameters with Gleason score and tumor angiogenesis. AJR Am J Roentgenol 2011;197:1382-90.

39. Chatterjee A, He D, Fan X, Wang S, Szasz T, Yousuf A, *et al.* Performance of ultrafast DCE-MRI for diagnosis of prostate cancer. Acad Radiol 2018;25:349-58.

40. Hötker AM, Mazaheri Y, Aras Ö, Zheng J, Moskowitz CS, Gondo T, *et al.* Assessment of prostate cancer aggressiveness by use of the combination of quantitative DWI and dynamic contrast-enhanced MRI. AJR Am J Roentgenol 2016;206:756-63.

41. Vos EK, Kobus T, Litjens GJ, Hambrock T, Hulsbergen-van de Kaa CA, Barentsz JO, *et al.* Multiparametric magnetic resonance imaging for discriminating low-grade from high-grade prostate cancer. Invest Radiol 2015;50:490-7.

42. Kobus T, Vos PC, Hambrock T, De Rooij M, Hulsbergen-Van de Kaa CA, Barentsz JO, *et al.* Prostate cancer aggressiveness: *In vivo* assessment of MR spectroscopy and diffusion-weighted imaging at 3 T. Radiology 2012;265:457-67.

43. Langer DL, van der Kwast TH, Evans AJ, Trachtenberg J, Wilson BC, Haider MA. Prostate cancer detection with multi-parametric MRI: Logistic regression analysis of quantitative T2, diffusion-weighted imaging, and dynamic contrast-enhanced MRI. J Magn Reson Imaging 2009;30:327-34.